A Comparative Investigation on the Use of Random Modulation Schemes for DC/DC Converters

K. K. Tse, Henry Shu-hung Chung, *Member, IEEE*, S. Y. R. Hui, *Senior Member, IEEE*, and H. C. So, *Member, IEEE*

***Abstract*—A comparative investigation on the use of random modulation schemes for dc/dc converters is presented. The modulation schemes under consideration include randomized pulse position modulation, randomized pulsewidth modulation (PWM), and randomized carrier-frequency modulation with fixed and variable duty cycle. The paper emphasizes the suitability and applicability of each scheme in dc/dc converters. Issues addressed include the effectiveness of randomness level on spreading the dominating frequencies that normally exist in constant-frequency PWM schemes, and the low-frequency power spectral density (PSD) of each scheme. The validity of the analyses is confirmed experimentally by using a dc/dc buck converter operating in continuous conduction mode. The PSD of the output under each scheme will be presented and compared.**

***Index Terms*—DC/DC power conversion, power electronics, pulsewidth modulation, random switching techniques, switching circuits.**

I. Introduction

With the introduction of the international electromagnetic compatibility (EMC) directives, there is an increasing awareness of the electromagnetic interference (EMI) problems of switched-mode power supplies (SMPS's) [1], [2]. The control of SMPS's is generally associated with the use of pulsewidth modulation (PWM) technique. During the last decade, random-switching technique, originated from statistical communication theory [3], has been applied to power electronics converters. Certain parameters that are named as stochastic variables in the PWM modulator are subject to randomization. The methodology is not merely a way to comply with the EMC regulations, but it also provides a flexible and practical approach to solving acoustic noise problems in inverter-based motor drives [4].

In conventional dc/dc converters, the output voltage is generally controlled by varying the duty cycle of the main switch. The duty cycle and switching frequency are kept constant in steady-state operation, so that the harmonic powers of the input current and output voltage are concentrated on the multiples of the switching frequency. Using various random switching schemes, the harmonic power in the frequency domain can be spread and the peak level of the power spectral density (PSD) becomes less than that of the classical PWM scheme. Discrete harmonics are significantly reduced and the harmonic power is spread over a continuous noise spectrum of small magnitude [5]. Spreading of harmonic energy across the spectrum may be carried out in various ways. Many randomization schemes and their syntheses have been addressed in many papers [5]–[7]. They can be categorized into four modulation schemes, including random pulse-position modulation (RPPM), random pulsewidth modulation (RPWM), and random carrier-frequency modulation with fixed duty cycle (RCFMFD), and with variable duty cycle (RCFMVD), respectively. However, the suitability and applicability of the use of random modulation schemes in dc/dc converters have not been addressed. It has been shown that random switching schemes could introduce an undesirable continuous noise spectrum within the passband of the low-pass filter in dc/dc converters, which requires tight output voltage regulation [8].

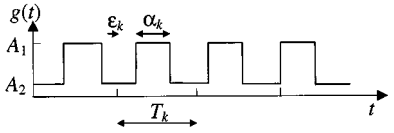

Fig. 1. Switching signal with randomized modulation scheme.

In this paper, a comparative investigation into the use of random modulation schemes in dc/dc converters is presented. The issues addressed include the effects of the stochastic variable randomness level on the PSD, low-frequency characterizations, and practicability of implementation of the above schemes, which are quantitatively investigated with uniform probability density distribution on the stochastic variable. Predictions are compared to measurements obtained in a dc/dc buck converter operating in continuous conduction mode (CCM).

II. Random Switching Schemes

A. Characteristics of Random Modulation Schemes

RPPM is similar to the classical PWM scheme with constant switching frequency. However, the position of the gate pulse is randomized within each switching period, instead of commencing at the start of each cycle. RPWM allows the pulsewidth to vary, but the average pulsewidth is equal to the required duty cycle. RCFMFD exhibits randomized switching period and constant duty cycle, while RCFMVD exhibits randomized switching period and constant pulsewidth. As the pulsewidth in RCFMVD is fixed and the switching period is randomized, the resultant duty cycle is also randomized. Nevertheless, the average duty cycle is equal to the desired value. With the aid of Fig. 1, the characteristics of the pulse in each scheme are summarized in Table I. $g(t)$ has two discrete levels (namely, A_1 and A_2), which are applicable to describe

Manuscript received September 1, 1998; revised May 16, 1999. Abstract published on the Internet December 23, 1999. This work was supported by the Hong Kong Research Grant Council.

The authors are with the Department of Electronic Engineering, City University of Hong Kong, Kowloon, Hong Kong.

Publisher Item Identifier S 0278-0046(00)02517-X.

the behaviors of classical dc/dc converters. T_k is the duration of the kth cycle. α_k is the duration of the gate pulse in the kth cycle. ϵ_k is the delay time of the gate pulse. d_k, which is equal to α_k/T_k, is the duty cycle of the switch in the kth cycle.

B. Definitions of the Randomness Level

In order to investigate the effectiveness of the stochastic variable randomness level on spreading harmonic power, a randomness level $\Re$ for each scheme is defined.

For RPPM,

$$\Re_{\mathrm{RPPM}} = \frac{\epsilon_2 - \epsilon_1}{T_S} \tag{1}$$

where $\epsilon_k \in [\epsilon_1, \epsilon_2]$. ϵ_1 and ϵ_2 are the minimum and maximum limits of the pulse position in each cycle. ϵ_1 is generally equal to zero. T_S is the nominal switching period.

For RPWM,

$$\Re_{\mathrm{RPWM}} = \frac{\alpha_2 - \alpha_1}{T_S} = d_2 - d_1 \tag{2}$$

where $\alpha_k \in [\alpha_1, \alpha_2]$. Thus, the duty cycle d_k varies between the minimum possible value d_1 and the maximum possible value d_2 around the nominal duty cycle in classical PWM scheme.

For RCFMFD and RCFMVD,

$$\Re_{\mathrm{RCFMFD}} = \Re_{\mathrm{RCFMVD}} = \frac{T_2 - T_1}{T_S}. \tag{3}$$

In these two modulation schemes, T_k varies between a minimum possible value T_1 and maximum possible value T_2. d_k in RCFMVD varies between $[(\alpha_k/T_2), (\alpha_k/T_1)]$, in which α_k is fixed.

C. PSD

The PSD $S_p(f, \Re)$ of the waveform in Fig. 1 with RPPM and RPWM can be shown [5] to be equal to

$$S_p(f,\Re) = f_S \left\{ E[\,|G(f)|^2] - |E[G(f)]|^2 + f_S |E[G(f)]|^2 \sum_{k=-\infty}^{\infty} \delta(f - k f_S) \right\} \tag{4}$$

where f_S is the nominal switching frequency and $G(f)$ is the Fourier transform of a cycle of $g(t)$ with randomness level $\Re$. $E[\cdot]$ is the expectation operator taking over the whole ensemble. For RPPM,

$$\begin{aligned} G(f) &= A_1 \int_{\epsilon_k}^{DT_S+\epsilon_k} e^{-j2\pi ft}\, dt \\ &\quad + A_2 \left(\int_0^{\epsilon_k} e^{-j2\pi ft}\, dt + \int_{DT_S+\epsilon_k}^{T_S} e^{-j2\pi ft}\, dt \right) \\ &= \frac{j}{2\pi f} \left[(A_1 - A_2)\left(e^{-j2\pi f DT_S} - 1\right) \right. \\ &\quad \left. \cdot e^{-j2\pi f \epsilon_k} + A_2 (e^{-j2\pi f T_S} - 1) \right]. \end{aligned} \tag{5}$$

TABLE I
CHARACTERISTICS OF DIFFERENT RANDOM SWITCHING SCHEMES

Switching schemes	T_k	α_k	ε_k	$d_k = \alpha_k / T_k$
Standard PWM	Fixed	Fixed	Zero	Fixed
RPPM	Fixed	Fixed	Randomized	Fixed
RPWM	Fixed	Randomized	Zero	Randomized
RCFMFD	Randomized	Randomized	Zero	Fixed
RCFMVD	Randomized	Fixed	Zero	Randomized

It is noted that ϵ_k is the random variable, having the probability density function $P(\epsilon_k)$. The expected value of $G(f)$ and $|G(f)|^2$ can be determined as the follows:

$$E[G(f)] = \int_{\epsilon_1}^{\epsilon_2} P(\epsilon_k) G(f)\, d\epsilon_k \tag{6}$$

$$E[\,|G(f)|^2] = \int_{\epsilon_1}^{\epsilon_2} P(\epsilon_k) G(f) G^*(f)\, d\epsilon_k \tag{7}$$

where $G^*(f)$ is the complex conjugate of $G(f)$, and $P(\epsilon_k)$ is in uniform distribution. That is,

$$P(\epsilon_k) = \frac{1}{\epsilon_2 - \epsilon_1} = \frac{1}{\Re_{\mathrm{RPPM}} T_S}. \tag{8}$$

By substituting (5) and (8) into (6) and (7),

$$\begin{aligned} E[\,|G(f)|^2] = \frac{2}{(2\pi f)^2} \Big\{ & (A_1 - A_2)^2 [1 - \cos(2\pi f D T_S)] \\ & + A_2^2 [1 - \cos(2\pi f T_S)] + \frac{A_2 (A_1 - A_2)}{2\pi f \Re_{\mathrm{RPPM}} T_S} \\ & \cdot [\sin(2\pi f D T_S) - \sin[2\pi f (D + \Re_{\mathrm{RPPM}}) T_S] \\ & + \sin(2\pi f \Re_{\mathrm{RPPM}} T_S) - 1 \\ & + \sin[2\pi f (1 - \Re_{\mathrm{RPPM}}) T_S] - \sin(2\pi f T_S) \\ & - \sin[2\pi f (1 - \Re_{\mathrm{RPPM}} - D) T_S] \\ & + \sin[2\pi f (1 - D) T_S] \Big\} \end{aligned} \tag{9}$$

$$\begin{aligned} E[G(f)] = \frac{1}{2\pi f} \Big[& \frac{A_1 - A_2}{2\pi f \Re_{\mathrm{RPPM}} T_S} \left(e^{-j2\pi f D T_S} - 1\right) \\ & \cdot \left(1 - e^{-j2\pi f \Re_{\mathrm{RPPM}} T_S}\right) \\ & + j A_2 (e^{-j2\pi f T_S} - 1) \Big] \end{aligned} \tag{10}$$

where D is the nominal duty cycle, and T_S is the nominal switching period.

For RPWM,

$$\begin{aligned} G(f) &= A_1 \int_0^{d_k T_S} e^{-j2\pi ft}\, dt + A_2 \int_{d_k T_S}^{T_S} e^{-j2\pi ft}\, dt \\ &= \frac{j}{2\pi f} \left[(A_1 - A_2) e^{-j2\pi f d_k T_S} - A_1 + A_2 e^{-j2\pi f T_S} \right] \end{aligned} \tag{11}$$

where d_k is considered as a random variable with $P(d_k)$ of uniform distribution. That is,

$$P(d_k) = \frac{1}{d_2 - d_1} = \frac{1}{\Re_{\mathrm{RPWM}}}. \tag{12}$$

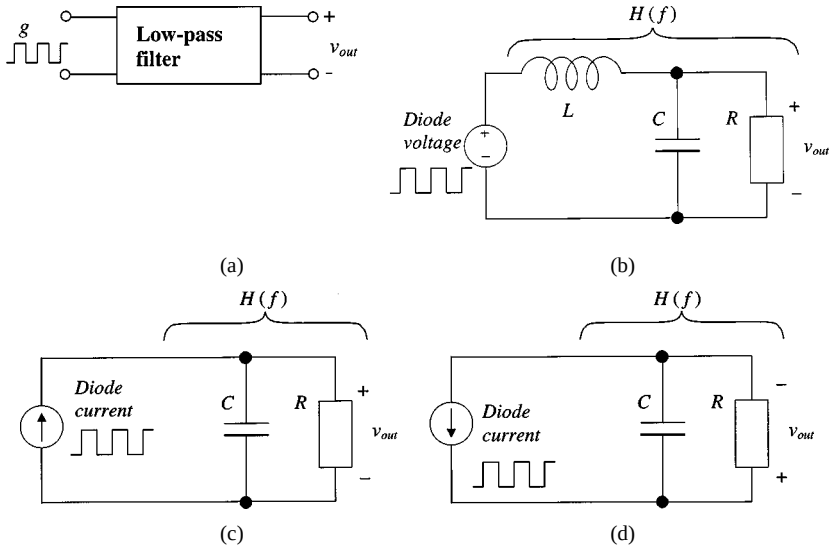

Fig. 2. Equivalent circuit of dc/dc converters. (a) Basic configuration. (b) Buck converter. (c) Boost converter. (d) Buck-boost converter.

TABLE II
TRANSFER CHARACTERISTICS OF VARIOUS DC/DC CONVERTERS

Converters	Source of g	$H(f)$
Buck	Diode voltage	$\frac{v_{out}}{v_D}(f)=\frac{1+2\pi f\, r_c C}{LC\left[j2\pi f(\frac{1}{RC}+\frac{r_L+r_c}{L})-(2\pi f)^2+\frac{1}{LC}(1+\frac{r_L}{R})\right]}$
Boost	Diode current	$\frac{v_{out}}{i_D}(f)=\frac{R(1+j2\pi f\, r_c C)}{1+j2\pi f(r_c+R)C}$
Buck-boost	Diode current	$\frac{v_{out}}{i_D}(f)=\frac{R(1+j2\pi f\, r_c C)}{1+j2\pi f(r_c+R)C}$

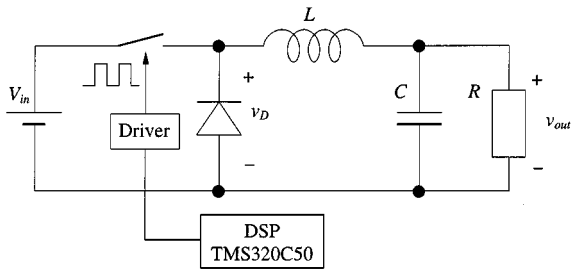

Fig. 3. Buck converter with the test setup.

Thus,

$$E[|G(f)|^2]=\int_{d_1}^{d_2}P(d_k)G(f)G^*(f)dd_k$$
$$=\frac{2}{(2\pi f)^2}\left\{A_1^2+A_2^2-A_1A_2\right.$$
$$\cdot[\cos(2\pi fT_S)+1]+\frac{A_2-A_1}{2\pi f\Re_{\mathrm{RPWM}}T_S}$$
$$\cdot\{A_1[\sin(2\pi fd_2T_S)-\sin(2\pi fd_1T_S)]$$
$$+A_2\{\sin[2\pi f(1-d_2)T_S]$$
$$\left.-\sin[2\pi f(1-d_1)T_S]\}\right\} \quad (13)$$

and

$$E[G(f)]=\int_{d_1}^{d_2}P(d_k)G(f)dd_k$$
$$=\frac{1}{2\pi f}\left[\frac{A_2-A_1}{2\pi f\Re_{\mathrm{RPWM}}T_S}\right.$$
$$\cdot(e^{-j2\pi fd_2T_S}-e^{-j2\pi fd_1T_S})$$
$$\left.+j(A_2e^{-j2\pi fT_S}-A_1)\right]. \quad (14)$$

The PSD's of RPPM and RPWM with randomness levels $\Re_{\mathrm{RPPM}}$ and $\Re_{\mathrm{RPWM}}$ can be obtained by substituting (9) and (10), and (13) and (14) into (4), respectively.

For RCFMFD and RCFMVD, the PSD can be shown to be equal to

$$S_p(f,\Re_{RCFM})=\frac{1}{E[T_k]}\left\{E[|G(f)|]^2\right.$$
$$\left.+2\,\mathrm{Re}\left\{\frac{E[G(f)e^{j2\pi fT_k}]E[G^*(f)]}{1-E[e^{j2\pi fT_k}]}\right\}\right\} \quad (15)$$

where $G^*(f)$ is the complex conjugate of $G(f)$. $P(T_k)$ is in uniform distribution. The proof of (15) is shown in the Appendix. The expected terms in (15) can be expressed as follows.

For RCFMFD, $G(f)$ is calculated with the constant duty cycle D and the randomized switching period T_k.

$$G(f)=A_1\int_0^{DT_k}e^{-j2\pi ft}\,dt+A_2\int_{DT_k}^{T_k}e^{-j2\pi ft}\,dt$$
$$=\frac{j}{2\pi f}\left[(A_1-A_2)e^{-j2\pi fDT_k}-A_1+A_2e^{-j2\pi fT_k}\right] \quad (16)$$

$$P(T_k)=\frac{1}{T_2-T_1}=\frac{1}{\Re_{\mathrm{RCFMFD}}T_S}. \quad (17)$$

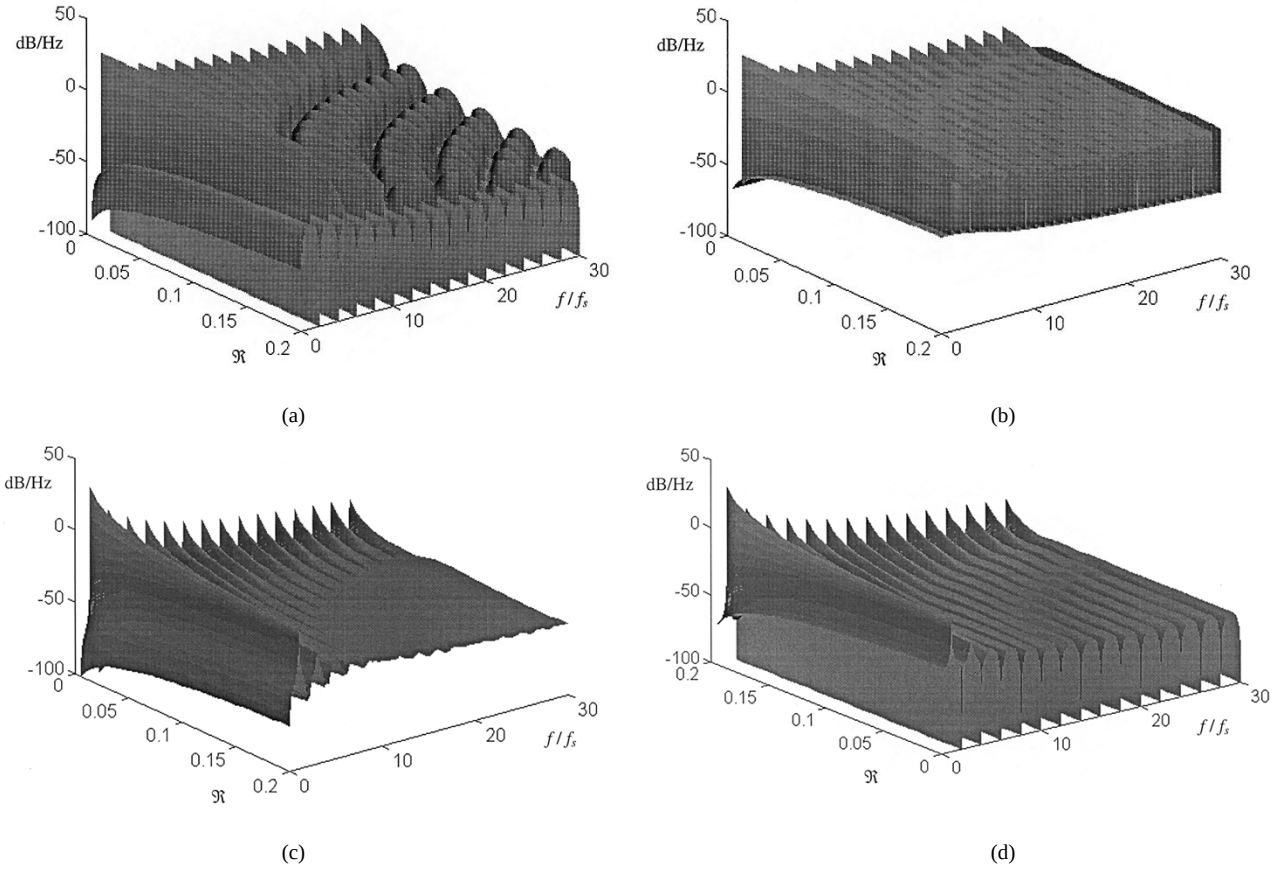

Fig. 4. PSD of the diode voltage with respect to the change in $\Re$ from 0 to 0.2. (a) RPPM. (b) RPWM. (c) RCFMFD. (d) RCFMVD.

Therefore,

$$\begin{aligned} E[\,|G(f)|^2] &= \int_{T_1}^{T_2} P(T_k)G(f)G^*(f)\,dT_k \\ &= \frac{2}{(2\pi f)^3 \Re_{\mathrm{RCFMFD}} T_S} \left\{ (A_2 - A_1) \right. \\ &\quad \cdot \left\{ \frac{A_1}{D} \left[\sin(2\pi f D T_2) - \sin(2\pi f D T_1)\right] \right. \\ &\quad - \frac{A_2}{1-D} \left\{\sin[2\pi f(1-D)T_2] \right. \\ &\quad \left. - \sin[2\pi f(1-D)T_1]\right\} \\ &\quad - A_1 A_2 [\sin(2\pi f T_2) - \sin(2\pi f T_1)] \\ &\quad \left. + 2\pi f \Re_{\mathrm{RCFMFD}} T_S (A_1^2 + A_2^2 - A_1 A_2) \right\} \end{aligned} \tag{18}$$

$$\begin{aligned} E[G(f)e^{j2\pi f T_k}] &= \int_{T_1}^{T_2} P(T_k)G(f)e^{j2\pi f T_k}\,dT_k \\ &= \frac{1}{(2\pi f)^2 \Re_{\mathrm{RCFMFD}} T_S} \left\{ \frac{A_1 - A_2}{1-D} \right. \\ &\quad \cdot [e^{j2\pi f(1-D)T_2} - e^{j2\pi f(1-D)T_1}] \\ &\quad - A_1 [e^{j2\pi f T_2} - e^{j2\pi f T_1}] \\ &\quad \left. + j A_2 2\pi f \Re_{\mathrm{RCFMFD}} T_S \right\} \end{aligned} \tag{19}$$

and

$$\begin{aligned} E[G^*(f)] &= \int_{T_1}^{T_2} P(T_k)G^*(f)\,dT_k \\ &= \frac{1}{(2\pi f)^2 \Re_{\mathrm{RCFMFD}} T_S} \left\{ \frac{A_1 - A_2}{D} \right. \\ &\quad \cdot [e^{j2\pi f D T_1} - e^{j2\pi f D T_2}] \\ &\quad - A_2 [e^{j2\pi f T_2} - e^{j2\pi f T_1}] \\ &\quad \left. + j A_1 2\pi f \Re_{\mathrm{RCFMFD}} T_S \right\} \end{aligned} \tag{20}$$

$$\begin{aligned} E[e^{j2\pi f T_k}] &= \int_{T_1}^{T_2} P(T_k) e^{j2\pi f T_k}\,dT_k \\ &= \frac{j}{2\pi f \Re_{\mathrm{RCFMFD}} T_S} (e^{j2\pi f T_1} - e^{j2\pi f T_2}). \end{aligned} \tag{21}$$

For RCFMVD, $G(f)$ is similar to (16) for RCFMFD but DT_k is a constant α. Hence,

$$G(f) = \frac{j}{2\pi f} \left[(A_1 - A_2)e^{-j2\pi f \alpha} - A_1 + A_2 e^{-j2\pi f T_k}\right]. \tag{22}$$

As $P(T_k)$ is in uniform distribution,

$$P(T_k) = \frac{1}{T_2 - T_1} = \frac{1}{\Re_{\mathrm{RCFMVD}} T_S}. \tag{23}$$

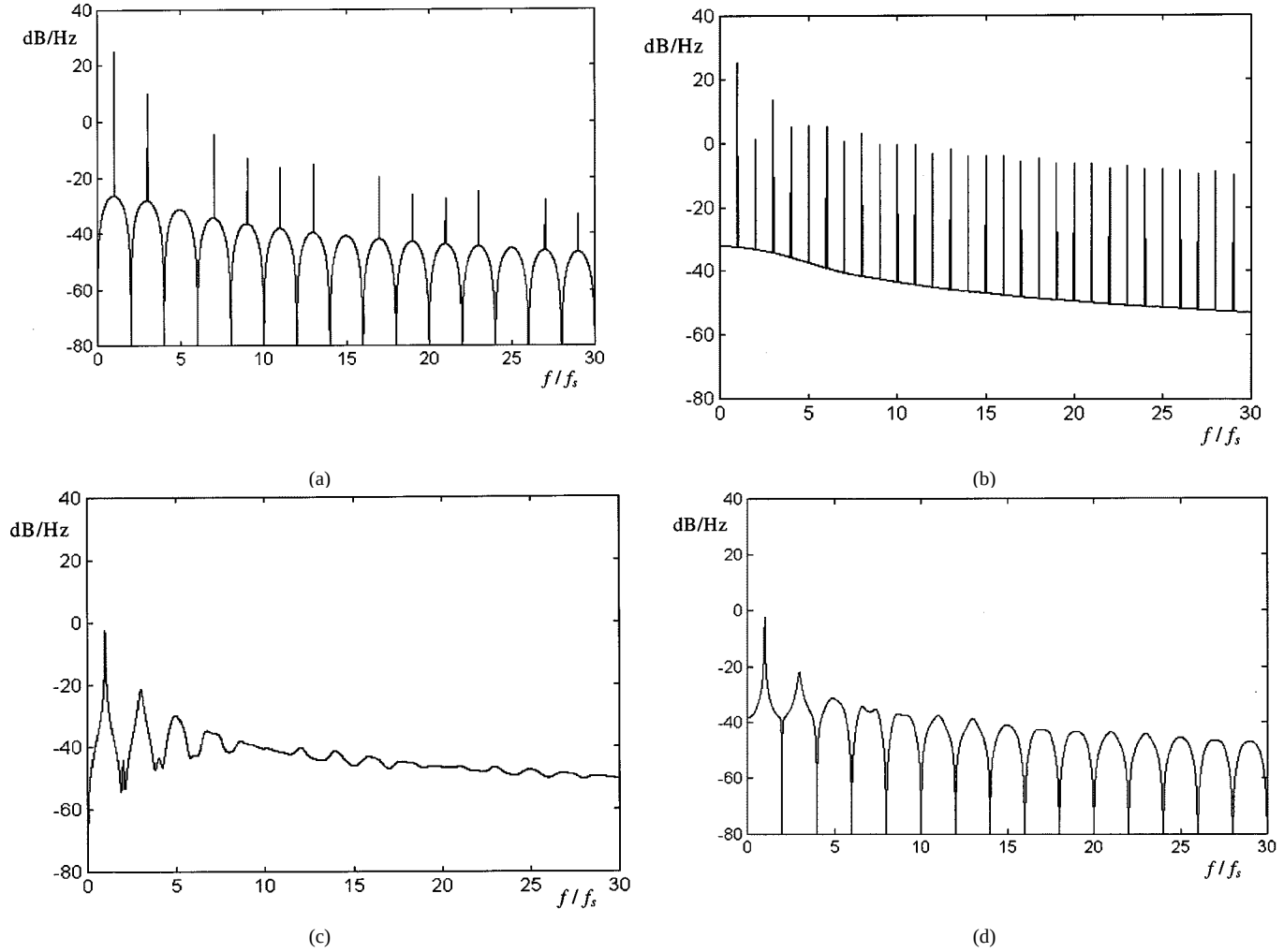

Fig. 5. PSD of the diode voltage with $\Re = 0.2$. (a) RPPM. (b) RPWM. (c) RCFMFD. (d) RCFMVD.

Then,

$$\begin{aligned} E[\,|G(f)|^2] &= \int_{T_1}^{T_2} P(T_k)G(f)G^*(f)\,dT_k \\ &= \frac{2}{(2\pi f)^3 \Re_{\mathrm{RCFMVD}} T_S}\,\{2\pi f \Re_{\mathrm{RCFMVD}} T_S \\ &\quad \cdot [A_1^2 + A_2^2 - A_1A_2 - A_1(A_1 - A_2) \\ &\quad \cdot \cos(2\pi f\alpha] - A_1A_2[\sin(2\pi fT_2) \\ &\quad - \sin(2\pi fT_1)] + A_2(A_1 - A_2) \\ &\quad \cdot \{\sin[2\pi f(T_2 - \alpha)] - \sin[2\pi f(T_1 - \alpha)]\}\} \end{aligned} \tag{24}$$

$$\begin{aligned} E[G(f)e^{j2\pi fT_k}] &= \int_{T_1}^{T_2} P(T_k)G(f)e^{j2\pi fT_k}\,dT_k \\ &= \frac{1}{(2\pi f)^2 \Re_{\mathrm{RCFMVD}} T_S} \\ &\quad \cdot \{[(A_1 - A_2)e^{-j2\pi f\alpha} - A_1](e^{j2\pi fT_2} \\ &\quad - e^{j2\pi fT_1}) + jA_2 2\pi f \Re_{\mathrm{RCFMVD}} T_S\} \end{aligned} \tag{25}$$

$$\begin{aligned} E[G^*(f)] &= \int_{T_1}^{T_2} P(T_k)G^*(f)\,dT_k \\ &= \frac{1}{(2\pi f)^2 \Re_{\mathrm{RCFMVD}} T_S}\,\{A_2[e^{j2\pi fT_1} \\ &\quad - e^{j2\pi fT_2}] + j2\pi f \Re_{\mathrm{RCFMVD}} T_S \\ &\quad \cdot [A_1 - (A_1 - A_2)e^{j2\pi f\alpha}]\} \end{aligned} \tag{26}$$

$$\begin{aligned} E[e^{j2\pi fT_k}] &= \int_{T_1}^{T_2} P(T_k)e^{j2\pi fT_k}\,dT_k \\ &= \frac{j}{2\pi f \Re_{\mathrm{RCFMVD}} T_S}\,[e^{j2\pi fT_1} - e^{j2\pi fT_2}]. \end{aligned} \tag{27}$$

Thus, the PSD's of RCFMFD and RCFMVD with randomness levels $\Re_{\mathrm{RCFMFD}}$ and $\Re_{\mathrm{RCFMVD}}$ can be obtained by substituting (18)–(21), and (24)–(27) into (15), respectively.

Comparing (4) and (15), the PSD's of RPPM and RPWM contain discrete harmonics at the multiples of f_S, while those in RCFMFD and RCFMVD show continuous spectrum.

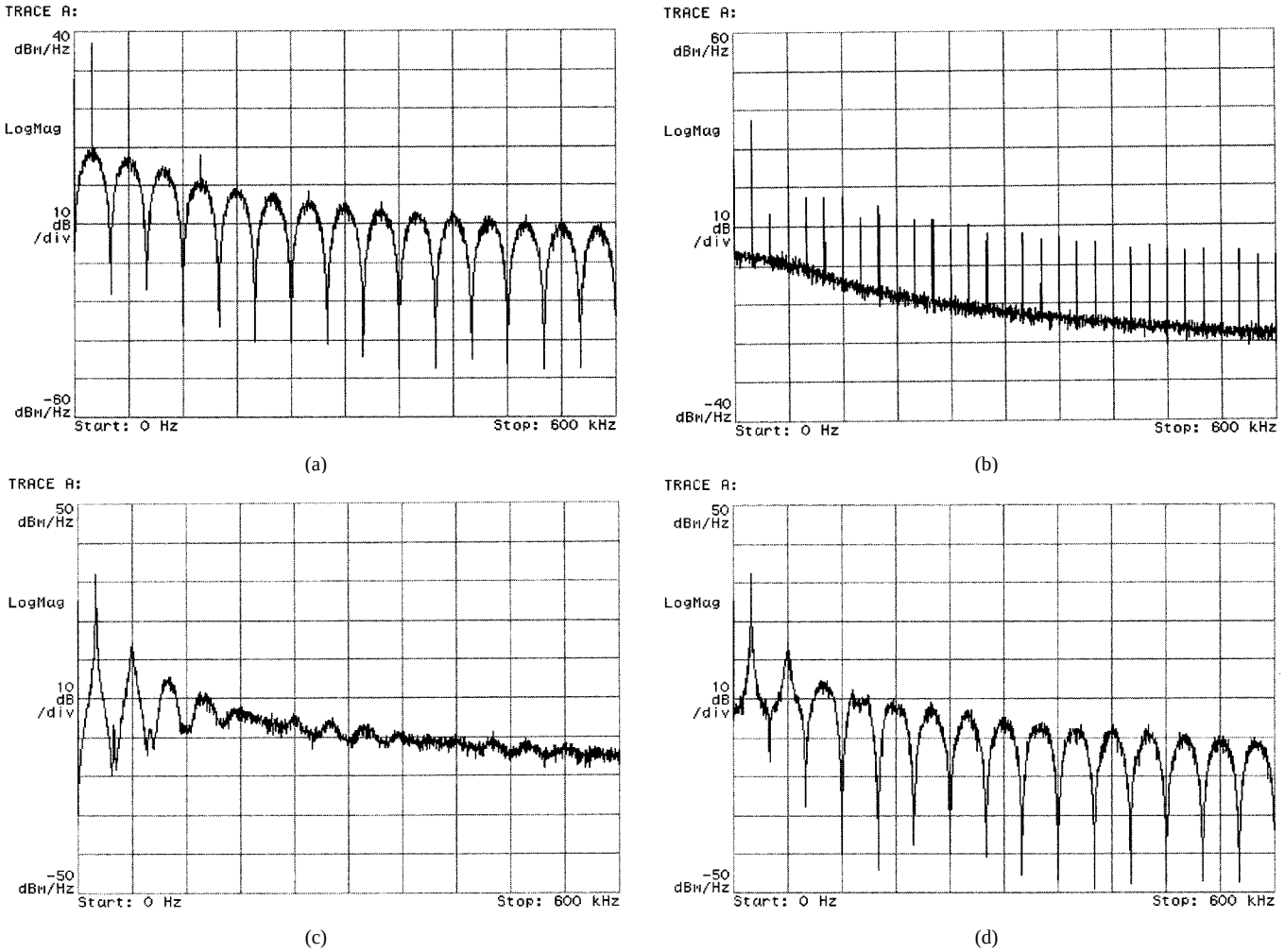

Fig. 6. Experimental PSD of the diode voltage with $\Re = 0.2$. (a) RPPM. (b) RPWM. (c) RCFMFD. (d) RCFMVD.

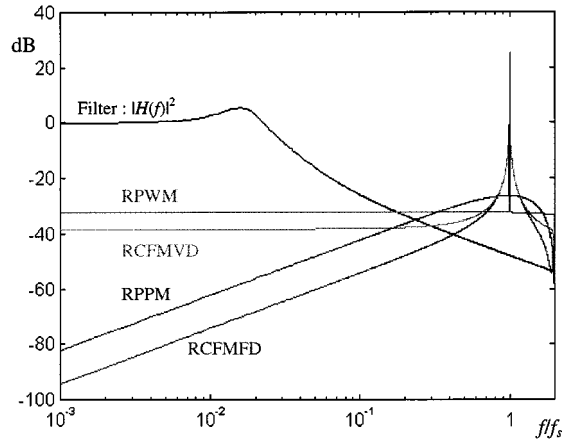

Fig. 7. Low-frequency characterizations with different random switching scheme.

D. Estimation of Output Noise Ripple

As shown in Fig. 2(a), a dc/dc converter is considered as a low-pass filter fed by different types of input sources, which are dependent on the circuit configuration. With the aid of Table II, the most common types of transformed dc/dc converters are illustrated in Fig. 2(b)–(d). Converters operating in CCM and having relatively constant inductor current are considered. Denote $H(f)$ as the transfer function of the filter. The PSD of the noise output of the converter can be shown to be [9]

$$S_{n_o}(f,\Re) = S_p(f,\Re)|H(f)|^2, \qquad f \neq 0. \tag{28}$$

The noise power is calculated by integrating $S_{n_o}(f,\Re)$ over the spectrum. Hence, the rms value of the noise ripple v_N in the converter output is

$$v_N(\Re) = \left[\int_{-\infty}^{\infty} S_p(f,\Re)|H(f)|^2\,df\right]^{1/2}, \qquad f \neq 0. \tag{29}$$

Due to the rapid roll-off characteristics in $|H(f)|^2$ at high-frequency range, v_N can be approximated by

$$v_N(\Re) = \left[2\int_{0}^{2f_S} S_p(f,\Re)|H(f)|^2\,df\right]^{1/2}, \qquad f \neq 0. \tag{30}$$

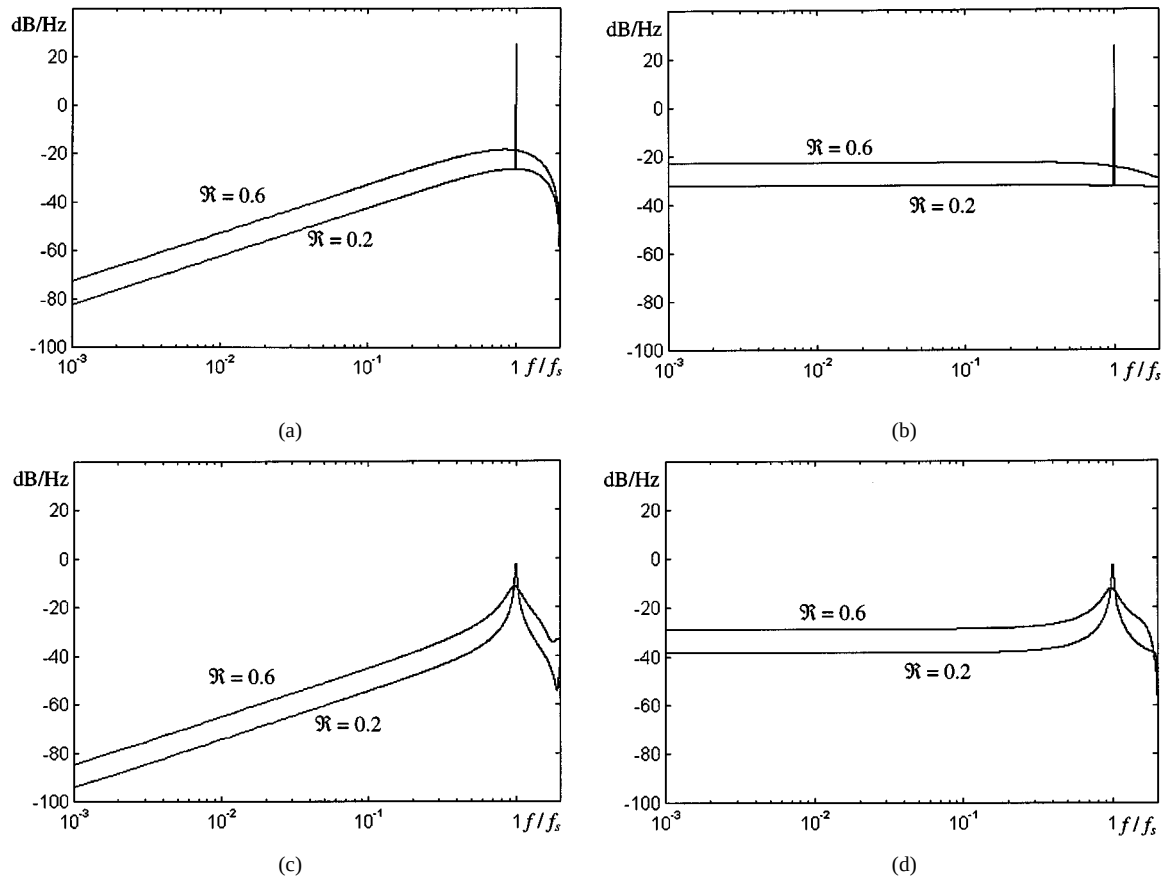

Fig. 8. Comparison of low-frequency characterizations with $\Re = 0.2$ and $\Re = 0.6$. (a) RPPM. (b) RPWM. (c) RCFMFD. (d) RCFMVD.

Since the $S_p(f, \Re)$ of RPPM and RPWM consists of continuous spectral component $[S_p^C(f, \Re)]$ and discrete spectral component $[S_p^D(f, \Re)]$, they can be expressed as

$$S_p^C[f, \Re) = f_S\{E[|G(f, \Re)|^2] - |E[G(f, \Re)]|^2\} \tag{31}$$

$$S_p^D(f, \Re) = f_S^2|E[G(f, \Re)]|^2. \tag{32}$$

v_N can be shown to be

$$v_N = \left[\frac{4f_S}{N}\sum_{k=1}^{N} S_p^C\left(\frac{2kf_S}{N}, \Re\right)\left|H\left(\frac{2kf_S}{N}\right)\right|^2 + S_p^D(f_S, \Re)|H(f_S)|^2\right]^{1/2} \tag{33}$$

where N is the number of frequency points over the range of $[0, 2f_s]$. For RCFMFD and RCFMVD, only the continuous component and the dc component exist over the spectrum. Thus,

$$v_N = \left[\frac{4f_S}{N}\sum_{k=1}^{N} S_p^C\left(\frac{2kf_S}{N}, \Re\right)\left|H\left(\frac{2kf_S}{N}\right)\right|^2\right]^{1/2}. \tag{34}$$

III. Experimental Verifications

A dc/dc buck converter is illustrated with a test setup as shown in Fig. 3. The component values are $L = 1$ mH, $r_L = 0.25\ \Omega$, $C = 220\ \mu$F, $r_C = 0.5\ \Omega$, and $R = 10\ \Omega$. The input voltage V_{in} is 60 V. The nominal switching frequency f_S is 20 kHz and the duty cycle is 0.5. The voltage waveform of D (i.e., v_D) is similar to the pulse train in Fig. 1 with $A_1 = V_{in}$ and $A_2 = 0$. The $H(f)$ of the output LC filter is (35), shown at the bottom of the next page.

Fig. 4 shows the variations of the PSD of v_D with respect to the changes in $\Re$ under the four random switching schemes. $\Re$ is changed from zero to 0.2. When $\Re$ equals zero, the PSD is the same as the PSD of the classical PWM scheme. As $\Re$ increases, the harmonic spectrum is gradually spread over. However, the PSD's of the RPPM and RPWM schemes consist of two components, namely, discrete components at the multiples of f_S and a continuous component over the frequencies. The PSD's of the RCFMFD and RCFMVD contain continuous spectrum only, because the switching frequency is randomized. Figs. 5 and 6 show the theoretical and experimental results of the PSD under the four schemes with $\Re = 0.2$. The measurements are obtained from a signal analyzer HP89410A with resolution bandwidth of 100 Hz. There is an overall 30-dB difference between the theoretical and experimental results. This difference is due to the fact that the analyzer gives the comparative results of the actual spectral power with 1 mW as reference. The unit of the theoretical spectral power is in decibels, while the measured one is in

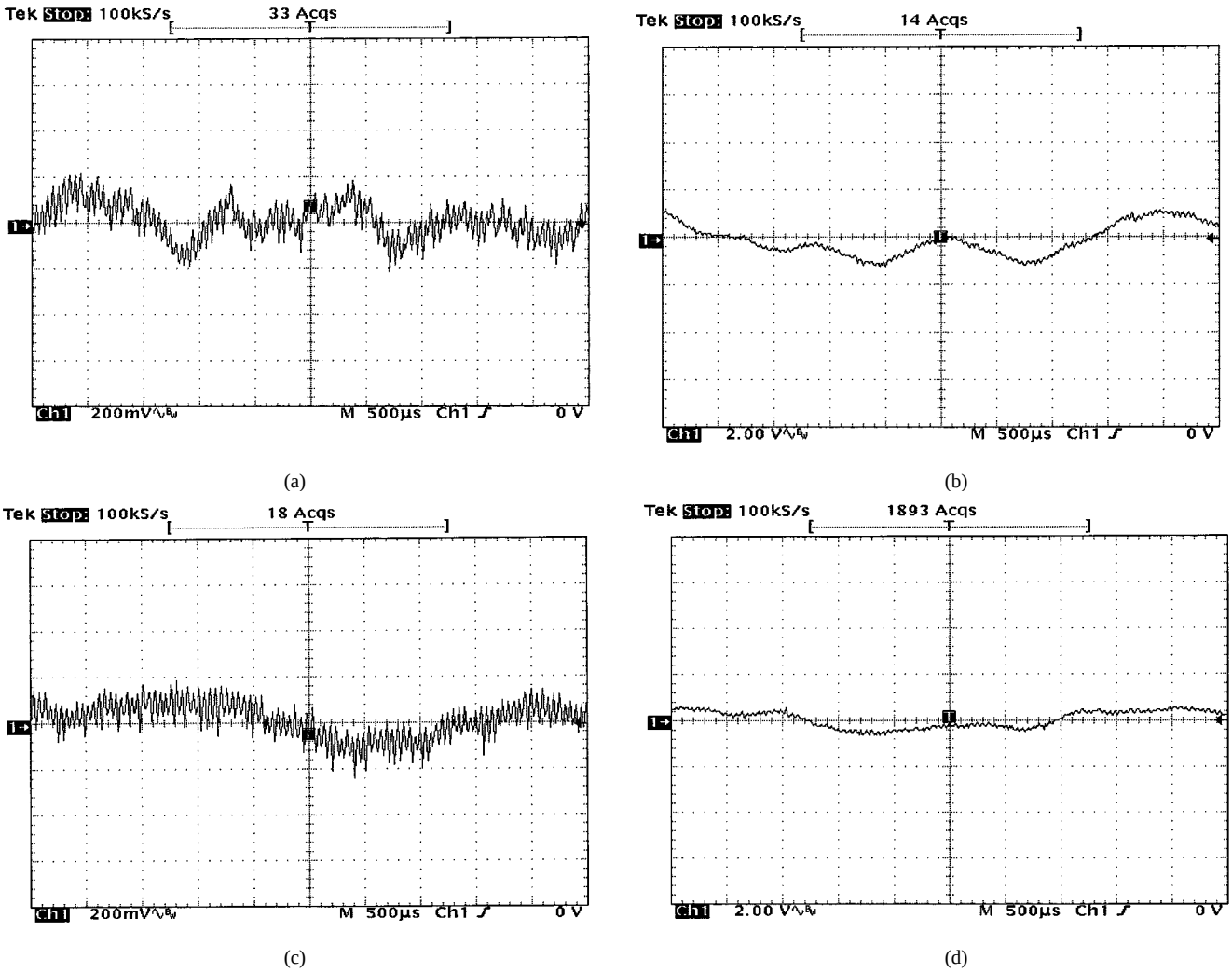

Fig. 9. Measured output noise ripples with different random switching scheme. (a) RPPM (200 mV/div). (b) RPWM (2 V/div). (c) RCFMFD (200 mV/div). (d) RCFMVD (2 V/div).

decibels referred to 1 mW. The relationship between these two units is demonstrated as follows. For instance, if the actual spectral power is P,

$$P_{\mathrm{dBm}} = 10\log\frac{P}{0.001} = 10\log P + 30\ \mathrm{dB} = P_{\mathrm{dB}} + 30\ \mathrm{dB}. \tag{36}$$

With the consideration of (36), the theoretical results show close agreement with the experimental ones. The low-frequency characterizations of v_D within the passband of the LC filter under the four schemes are shown in Fig. 7. It can be observed that RCFMFD introduces the lowest low-frequency harmonic spectrum. RCFMFD combines the advantages of: 1) spreading harmonic power at the multiples of the switching frequency and 2) not introducing significant disturbances at the low-frequency range. The main reason for this feature is that the duty cycle in every switching cycle is constant, even if the switching frequency is varied, giving a relatively stable output voltage. This factor can be observed from the behaviors of RPWM and RCFMVD schemes, in which relatively large low-frequency voltage variations are present because of the varying duty cycle. The duty cycle in the two schemes is changing because the pulsewidth is randomized in RPWM and the switching period is randomized in RCFMVD. Although the average duty cycle in RPPM is constant, the actual ratio between the on time and off time of S in every switching cycle is randomized. Thus, the low-frequency harmonic components are higher than those

$$H(f) = \frac{1 + 2\pi f r_C C}{LC\left[j2\pi f\left(\frac{1}{RC} + \frac{r_L + r_C}{L}\right) - (2\pi f)^2 + \frac{1}{LC}\left(1 + \frac{r_L}{R}\right)\right]} \tag{35}$$

of RCFMFD. From the above observations, RCFMFD offers the best spectral characteristics in dc/dc converter applications among the random schemes under consideration.

As shown in Fig. 4, no significant enhancements in spreading high-frequency harmonics are observed when $\Re$ is larger than 0.15 for the four schemes. However, low-frequency harmonic components increase as $\Re$ increases. Fig. 8 shows the low-frequency characterization of v_D under the four switching schemes with $\Re$ equal to 0.2 and 0.6, respectively. It can be observed that the low-frequency harmonics within the passband of the output filter are generally increased when $\Re$ increases. When $\Re$ becomes unnecessarily large (say $\Re > 0.2$), the advantage of reducing discrete harmonic components is offset by the increase in the low-frequency output ripple.

Fig. 9 shows the measured output ripple voltage of the converter under the four switching schemes. The RCFMFD gives the lowest ripple voltage. Take $N = 1000$, by using (33) and (34), the computed v_N is 0.13 V in the RPPM scheme, 1.08 V in the RPWM scheme, 0.55 V in the RCFMVD scheme, and 0.11 V in the RCFMFD scheme. These predictions are in close agreement with the experimental measurements.

IV. Conclusions

This paper has given a comparative investigation into the effects of the randomness level on the PSD of four random modulation schemes that are applied to classical dc/dc converters operating in CCM and having relatively constant inductor current. It has been demonstrated that, by controlling the degree of randomness, all schemes can gradually spread the discrete frequency harmonic power over the frequency spectrum. However, the continuous noise spectrum within the passband of the low-pass filter results in a noise-induced low-frequency ripple in the converter output voltage. This investigation shows that among all random schemes under consideration, the RCFMFD gives the minimum low-frequency harmonic spectrum and is, therefore, considered as the best choice for dc/dc converter applications. Further research will be dedicated to a comprehensive study of RCFMFD in suppressing conducted EMI in an offline switching-mode power supply and an investigation of converters operating in discontinuous conduction mode.

Appendix

A. Proof of (15)

Considering a generic switching cycle k in Fig. 1, the switching waveform $g_k(t-t_k)$, can be expressed as

$$g_k(t-t_k) = \begin{cases} A1, & \text{for } t_k \le t < DT_k \\ A2, & \text{for } DT_k \le t < T_k \\ 0, & \text{elsewhere} \end{cases} \tag{A.1}$$

where T_k is a randomized switching period in theRCFMFD and RCFMVD schemes. For RCFMVD, α_k is fixed and D is varied. A general expression for $g(t)$ is

$$g(t) = \lim_{N\to\infty} \sum_{k=1}^{N} g_k(t-t_k). \tag{A.2}$$

The autocorrelation of $g(t)$ is defined as

$$R_g(\tau) = E\left[\lim_{T_o\to\infty} \frac{1}{T_o} \int_0^{T_o} g(t)g(t+\tau)\,dt\right] \tag{A.3}$$

where $E[\cdot]$ is the expected value of the quantity inside the bracket. T_o is the observation interval, containing N expected value of T_k. That is,

$$T_o = NE[T_k]. \tag{A.4}$$

By substituting (A.2) and (A.4) into (A.3),

$$R_g(\tau) = \lim_{N\to\infty} \frac{1}{NE[T_k]} \sum_{k=1}^{N}\sum_{l=1}^{N} \cdot E\left[\int_0^{\infty} g_k(t-t_k)g_l(t+\tau-t_l)\,dt\right]. \tag{A.5}$$

If $G_k(f)$ and $G_l(f')$ denote the Fourier transform of $g_k(t)$ and $g_l(t)$, respectively, and Γ denotes the time integral in (A.5),

$$\begin{aligned}\Gamma &= \int_0^{\infty} g_k(t-t_k)g_l(t+\tau-t_1)\,dt \\ &= \int_0^{\infty} \left[\int_{-\infty}^{\infty} G_k(f)e^{-j2\pi f t_k}e^{j2\pi f t}\,df\right] \\ &\quad \cdot \left[\int_{-\infty}^{\infty} G_l(f')e^{j2\pi f'(\tau-t_l)}e^{j2\pi f' t}\,df'\right]\,dt \\ &= \int_0^{\infty}\int_{-\infty}^{\infty}\int_{-\infty}^{\infty} e^{j2\pi(f+f')t}\,dt\,G_k(f)G_l(f') \\ &\quad \cdot e^{-j2\pi f t_k}e^{j2\pi f'(\tau-t_l)}\,df\,df'. \end{aligned} \tag{A.6}$$

Referring to [3],

$$\int_{-\infty}^{\infty} e^{j2\pi(f+f')t}\,dt = \delta(f'+f). \tag{A.7}$$

Equation (A.6) can be expressed as

$$\begin{aligned}\Gamma &= \int_0^{\infty}\int_{-\infty}^{\infty} \delta(f'+f)G_k(f)G_l(f') \\ &\quad \cdot e^{-j2\pi f t_k}e^{j2\pi f'(\tau-t_l)}\,df\,df' \\ &= \int_0^{\infty} G_k(-f')G_l(f')e^{j2\pi f'\tau}e^{j2\pi f'(t_k-t_l)}\,df' \\ &= \int_0^{\infty} G_k^*(f)G_l(f)e^{j2\pi f\tau}e^{j2\pi f(t_k-t_l)}\,df. \end{aligned} \tag{A.8}$$

Hence, the autocorrelation of g can be expressed as

$$R_g(\tau) = \lim_{N\to\infty} \frac{1}{NE[T_k]} \sum_{k=1}^{N}\sum_{l=1}^{N} \int_0^{\infty} E[G_l(f)G_k^*(f) \cdot e^{j2\pi f(t_k-t_l)}]e^{j2\pi f\tau}\,df. \tag{A.9}$$

Based on the Wiener–Khinchin theorem [3], the PSD of a signal $S(f)$ is the Fourier transform of its autocorrelation func-

tion $R(\tau)$. Conversely, the autocorrelation can be given by the inverse Fourier transform of the PSD. That is,

$$S(f) = \int_{-\infty}^{\infty} R(\tau) e^{-j2\pi f\tau}\, d\tau \tag{A.10}$$

and

$$R(\tau) = \int_{-\infty}^{\infty} S(f) e^{j2\pi f\tau}\, df. \tag{A.11}$$

With this relationship, the PSD of g over the range of positive frequency, $S_p(f, \Re_{RCFM})$, is easily observed from (A.9), in terms of the randomness level of T_k, i.e.,

$$S_p(f,\Re_{RCFM}) = \lim_{N\to\infty} \frac{1}{NE[T_k]} \sum_{k=1}^{N}\sum_{l=1}^{N} \cdot E[G_l(f)G_k^*(f)e^{j2\pi f(t_k - t_l)}]. \tag{A.12}$$

Consider $S_\Sigma(f)$ denoting the double summation of the expected term in (A.12)

$$S_p(f,\Re_{RCFM}) = \lim_{N\to\infty} \frac{1}{NE[T_k]} S_\Sigma(f), \tag{A.13}$$

where

$$\begin{aligned} S_\Sigma(f) &= \sum_{k=1}^{N}\sum_{l=1}^{N} E[G_l(f)G_k^*(f)e^{j2\pi f(t_k-t_l)}] \\ &= NE[\,|G(f)|^2] + \sum_{k=1}^{N}\sum_{\substack{l=1\\ l\neq k}}^{N} \cdot E[G_l(f)G_k^*(f)e^{j2\pi f(t_k-t_l)}] \end{aligned} \tag{A.14}$$

$G_l(f)$ is dependent on $e^{j2\pi f(t_k-t_l)}$ if

$$|t_k - t_l| = T_l \tag{A.15}$$

and $G_k^*(f)$ is dependent on $e^{j2\pi f(t_k-t_l)}$ if

$$|t_k - t_l| = T_k. \tag{A.16}$$

Hence, (A.14) can be shown to be

$$\begin{aligned} S_\Sigma(f) = {} & NE[\,|G(f)|^2] + 2(N-1) \\ & \cdot \mathrm{Re}\{E[G(f)]E[G^*(f)e^{j2\pi f T_k}]\} \\ & + \Phi_\Sigma(f) \end{aligned} \tag{A.17}$$

where

$$\begin{aligned} \Phi_\Sigma(f) = {} & G_1^*(f)\sum_{l=3}^{N} G_l(f)e^{j2\pi f(t_1-t_l)} \\ & + G_2^*(f) \sum_{\substack{l=4\\ l\neq 1,2,3}}^{N} G_l(f)e^{j2\pi f(t_2-t_l)} \\ & + G_3^*(f) \sum_{\substack{l=1\\ l\neq 2,3,4}}^{N} G_l(f)e^{j2\pi f(t_3-t_l)} \\ & + \cdots + G_N^*(f)\sum_{l=1}^{N-2} G_l(f)e^{j2\pi f(t_N-t_l)}. \end{aligned} \tag{A.18}$$

Consider

$$\phi = E[e^{j2\pi f T_k}] \tag{A.19}$$

and

$$E[e^{j2\pi f(t_k-t_l)}] = \begin{cases} [\phi]^{k-l}, & \text{for } k > l \\ [\phi^*]^{l-k}, & \text{for } l > k. \end{cases} \tag{A.20}$$

Thus, (A.18) becomes a real number as

$$\begin{aligned} \Phi_\Sigma(f) = {} & 2\mathrm{Re}\{E[G^*(f)]E[G(f)e^{j2\pi f T_k}] \\ & \cdot (\phi + \phi + \phi^2 + \phi + \phi^2 + \phi^3 + \cdots + \phi \\ & + \phi^2 + \phi^3 + \phi^4 + \cdots + \phi^{N-2})\}. \end{aligned} \tag{A.21}$$

Since $|\phi| < 1$, (A.21) is simplified as

$$\begin{aligned} \Phi_2(f) = {} & 2\mathrm{Re}\left\{E[G^*(f)]E[G(f)]E[G(f)e^{j2\pi f T_k}]\right. \\ & \left. \cdot \frac{\phi}{1-\phi}\left[(N-1) - \frac{1-\phi^{N-1}}{1-\phi}\right]\right\}. \end{aligned} \tag{A.22}$$

By substituting (A.22) into (A.17),

$$\begin{aligned} S_\Sigma(f) = {} & NE[\,|G(f)|^2] + 2(N-1) \\ & \cdot \mathrm{Re}\left\{E[G^*(f)]E[G(f)e^{j2\pi f T_k}]\left(1 + \frac{\phi}{1-\phi}\right)\right\} \\ & + 2\mathrm{Re}\left\{E[G^*(f)]E[G(f)e^{j2\pi f T_k}]\right. \\ & \left. \cdot \frac{\phi(1-\phi^{N-1})}{(1-\phi)^2}\right\}. \end{aligned} \tag{A.23}$$

Finally, (A.13) becomes

$$\begin{aligned} S_p(f,\Re_{RCFM}) = {} & \frac{1}{E[T_k]}\left(E[\,|G(f)|^2] + 2\,\mathrm{Re}\right. \\ & \left. \cdot \left[\frac{E[G(f)e^{j2\pi f T_k}]E[G^*(f)]}{1 - E[e^{j2\pi f T_k}]}\right]\right). \end{aligned} \tag{A.24}$$

REFERENCES

[1] F. Lin and D. Y. Chen, "Reduction of power supply EMI emission by switching frequency modulation," *IEEE Trans. Power Electron.*, vol. 9, pp. 132–137, Jan. 1994.

[2] D. Stone and B. Chambers, "The effects of carrier frequency modulation of PWM waveforms on conducted EMC problems in switched mode power supplies," *EPE J.*, vol. 5, no. 3/4, pp. 32–37, Jan. 1996.

[3] D. Middleton, *An Introduction to Statistical Communication Theory*. New York: McGraw-Hill, 1996.

[4] T. G. Habetler and D. M. Divan, "Acoustic noise reduction in sinuosidal PWM drives using a randomly modulated carrier," *IEEE Trans. Power Electron.*, vol. 6, pp. 356–363, July 1991.

[5] A. M. Stankovic, G. C. Verghese, and D. J. Perreault, "Analysis and synthesis of randomised modulation schemes for power converters," *IEEE Trans. Power Electron.*, vol. 10, pp. 680–693, Nov. 1995.

[6] T. Tanaka, K. Harada, and T. Ninomiya, "Noise analysis of dc-to-dc converter with random switching control," in *Proc. INTELEC'91*, Nov. 1991, pp. 283–290.

[7] T. Tanaka, T. Ninomiya, and K. Harada, "Random switching control in dc-dc converters," in *Proc. IEEE PESC'89*, 1989, pp. 500–507.

[8] Y. Shrivastava, S. Y. R. Hui, S. Sathiakumar, H. Chung, and K. K. Tse, "Effects of continuous noise in randomised switching dc-dc converters," *Electron. Lett.*, vol. 33, no. 11, pp. 919–921, 1997.

[9] A. Papoulis, *Probability Random Variables, and Stochastic Processes*. New York: McGraw-Hill, 1991.

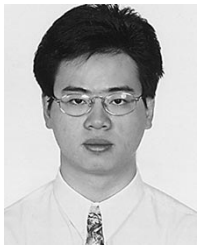

K. K. Tse received the B.Eng. (Hons.) degree in electrical engineering from The Hong Kong Polytechnic University, Hong Kong, in 1995 and the Ph.D. degree from the Department of Electronic Engineering, City University of Hong Kong, Hong Kong, in 2000.

He is currently a Research Fellow in the Department of Electronic Engineering, City University of Hong Kong. He has authored several technical papers on his research interests, which include computer-aided simulation technique, numerical modeling methods, EMI reduction, and random switching schemes for dc–dc converters.

Dr. Tse was awarded the First Prize in the 1998 IEEE Postgraduate Student Paper Contest, IEEE Hong Kong Section, and Third Prize in the 1998 IEEE Region 10 Postgraduate Student Paper Contest.

Henry Shu-hung Chung (S'92–M'95) received the B.Eng. degree (with first class honors) in electrical engineering and the Ph.D. degree from The Hong Kong Polytechnic University, Hong Kong, in 1991 and 1994, respectively.

Since 1995, he has been with City University of Hong Kong, Kowloon, Hong Kong, where he is currently an Associate Professor in the Department of Electronic Engineering. His research interests include time- and frequency-domain analysis of power electronics circuits, switched-capacitor-based converters, random-switching techniques, digital audio amplifiers, fuzzy logic control, and soft-switching converters. He has authored more than 105 technical papers, including 47 refereed journal publications. He is currently Chairman of the Council of the Sir Edward Youde Scholar's Association.

Dr. Chung was the recipient of the China Light and Power Prize and was awarded the Scholarship and Fellowship of the Sir Edward Youde Memorial Fund in 1991 and 1993, respectively. He is currently the IEEE Student Branch Counselor, City University of Hong Kong. He was Track Chair of the Technical Committee on Power Electronics Circuits and Power Systems of the IEEE Circuits and Systems Society in 1997–1998. He is currently an Associate Editor of the IEEE TRANSACTIONS ON CIRCUITS AND SYSTEMS—I: FUNDAMENTAL THEORY AND APPLICATIONS. He has also been listed in *Marquis Who's Who in the World*.

S. Y. (Ron) Hui (SM'94) was born in Hong Kong in 1961. He received the B.Sc.(Hons.) degree from the University of Birmingham, Birmingham, U.K., in 1984, and the D.I.C. and Ph.D degrees from Imperial College of Science, Technology and Medicine, London, U.K., in 1987.

He was a Lecturer in power electronics at the University of Nottingham, Nottingham, U.K., in 1987–1990. In 1990, he took up a Lectureship at the University of Technology, Sydney, Australia, where he became a Senior Lecturer in 1991. Later, he joined the University of Sydney, Sydney, Australia, and was promoted to Reader of Electrical Engineering and Director of the Power Electronics and Drives Research Group in 1996. He is currently a Chair Professor of Electronic Engineering, City University of Hong Kong, Kowloon, Hong Kong. He has authored more than 130 published technical papers, including more than 70 refereed journal publications. His research interests include all aspects of power electronics.

Prof. Hui is a Fellow of the Institution of Electrical Engineers, U.K., Institution of Electrical Engineers (Australia), and Hong Kong Institution of Electrical Engineers. He is an Associate Editor of the IEEE TRANSACTIONS ON POWER ELECTRONICS.

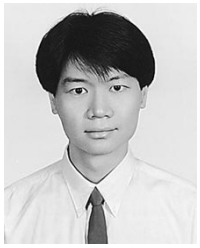

H. C. So (S'90–M' 90) was born in Hong Kong in 1968. He received the B.Eng. degree from City Polytechnic of Hong Kong, Hong Kong, and the Ph.D. degree from the Chinese University of Hong Kong, Hong Kong, in 1990 and 1995, respectively, both in electronic engineering.

From 1990 to 1991, he was an Electronic Engineer in the Research and Development Division, Everex Systems Engineering Ltd. During 1995–1996, he was a Post-Doctoral Fellow at the Chinese University of Hong Kong. He is currently a Research Assistant Professor in the Department of Electronic Engineering, City University of Hong Kong, Hong Kong. His research interests include adaptive signal processing, detection and estimation, source localization, and wavelet transform.